Biochemical Pharmacology, Vol. 56, pp. 1645–1656, 1998.

ISSN 0006-2952/98/$–see front matter
PII S006-2952(98)00275-5

Neuroprotective Activities of Carvedilol and a Hydroxylated Derivative

Role of Membrane Biophysical Interactions

Paul G. Lysko,† Kathryn A. Lysko,* Christine L. Webb,* Giora Feuerstein,* Pamela E. Mason,‡ Mary F. Walter‡ and R. Preston Mason‡*

*Department of Cardiovascular Pharmacology, SmithKline Beecham Pharmaceuticals, King of Prussia, PA; and ‡Membrane Biophysics Laboratory, Cardiovascular and Pulmonary Research Institute, Allegheny University of the Health Sciences, Allegheny Campus, Pittsburgh, PA, U.S.A.

ABSTRACT. Carvedilol is a vasodilating β-blocker and antioxidant approved for treatment of mild to moderate hypertension, angina, and congestive heart failure. SB 211475 (4-[2-hydroxyl-3-[[2-(2-methoxy-phenoxy)ethyl]amino]propoxyl]-9*H*-carbazol-3-ol), a hydroxylated carvedilol analogue, is an even more potent antioxidant in several assay systems. Carvedilol also has neuroprotective capacity with modulatory actions at *N*-methyl-D-aspartate (NMDA) receptors and Na^+ channels. In the present study, we demonstrated that in cultured rat cerebellar neurons, SB 211475 has 28-fold greater antioxidant activity than carvedilol, but is 2- to 6-fold less potent, respectively, at inhibiting neurotoxic activities at Na^+ channels and at NMDA receptor channels. To determine a biophysical rationale for these differential activities, small angle x-ray scattering data were obtained from model lipid and brain membrane bilayers containing either carvedilol, SB 211475, or dihydropyridine calcium channel blockers. Electron density profiles revealed that the location of SB 211475 was restricted to the glycerol backbone/hydrocarbon interface and significantly reduced membrane width by 5%, whereas the time-averaged location for carvedilol and flunarizine also extended to the hydrated surface of the bilayer. Comparison of carvedilol with several dihydropyridines showed a correlation between high ClogP values (lipophilicity), Na^+ channel inhibitory potency, and bilayer localization. The antioxidant activity of SB 211475 could be explained by restricted intercalation into the glycerol phosphate/hydrocarbon interface, creating an increase in volume associated with the phospholipid acyl chains, which would then become resistant to lipid peroxidation. Differential channel modulation may also be explained by these membrane structural results, which indicate that carvedilol and the less spatially restricted dihydropyridine molecules are more likely to inhibit transmembrane receptor channels. BIOCHEM PHARMACOL **56**;12:1645–1656, 1998. © 1998 Elsevier Science Inc.

KEY WORDS. cerebellar neuron; x-ray scatter; antioxidant; NMDA; sodium channel; dihydropyridine

Carvedilol, a novel, multiple-action neurohormonal antagonist, has been shown to have greater cardioprotective efficacy than other β-blockers in animal models of cardiac ischemia [1]. Carvedilol has also been shown to scavenge oxygen free radicals and inhibit lipid peroxidation in swine heart [2]. The capacity of carvedilol to scavenge oxygen free radicals in both lipid and aqueous environments has been confirmed using electron spin traps to generate EPR spectra [3, 4]. Carvedilol produced a concentration-dependent decrease in the intensity of the EPR signals formed in the presence of a cell-free oxygen radical generating system; other β-blockers were ineffective. SB 211475 (4-[2-hydroxyl-3-[[2-(2-methoxy-phenoxy)ethyl]amino]propoxyl]-9*H*-carbazol-3-ol), the 3-hydroxylated analogue of carvedilol (Fig. 1), has been shown to be an exceptionally potent antioxidant in a postischemic rat heart model, where its protective action may be mediated primarily through a lipid peroxidation chain-breaking mechanism [5]. Because oxygen free radicals have been implicated in cerebral ischemia and injury as well as in myocardial damage, we have explored the additional therapeutic potential of carvedilol within the central nervous system. We have studied the ability of carvedilol to scavenge oxygen free radicals and inhibit lipid peroxidation in rat brain membranes, and have found a potency two orders of magnitude greater than that seen for other β-blockers [3]. Similarly, carvedilol prevents Fe^{2+}/vitamin C-induced depletion of α-tocopherol from brain homogenates, while other β-blockers do not [3]. SB 211475 has been found to be much more potent than carvedilol and other antioxidants against lipid peroxidation in rat brain homogenates, and it protects many cell types from free radical damage [6]. With structure–activity relationship studies, we determined that the antioxidant effect of carvedilol resides within the carbazole moiety (Fig. 1) and is enhanced markedly (10- to 40-fold) by hydroxylation

† Corresponding author: Paul G. Lysko, Ph.D., Department of Cardiovascular Pharmacology, P.O. Box 1539, UW2510, King of Prussia, PA 19406-0939. Tel. (610) 270-6201; FAX (610) 270-5080; E-mail: Paul_G_Lysko@sbphrd.com

Received 18 August 1997; accepted 9 July 1998.

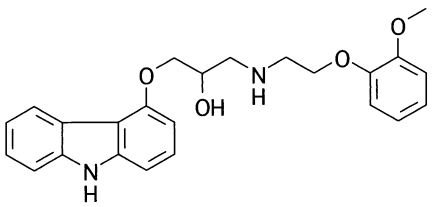

CARVEDILOL

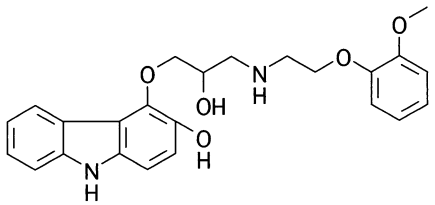

SB 211475

FIG. 1. Structures of carvedilol and SB 211475. SB 211475 (4-[2-hydroxyl-3-[[2-(2-methoxy-phenoxy)ethyl]amino] propoxyl]-9*H*-carbazol-3-ol) differs from carvedilol by being hydroxylated at the 3 position of the carbazole ring.

of the carbazole ring [3]. A solid correlation between IC_{50} values for lipid peroxidation and their oxidation potentials showed that these compounds are effective reducing agents, with the tendency to donate electrons and nullify toxic oxygen free radicals.

To determine whether carvedilol provided neuroprotection in ischemic brain as well as in heart, we further studied this potential in a model of gerbil forebrain ischemia where animals were exposed to 6 min of bilateral carotid artery occlusion. Seven days after ischemia, 52% protection of CA1 hippocampal neurons was achieved by both pretreatment and posttreatment with subcutaneous injections of carvedilol [7]. To explore the potential molecular mechanisms of carvedilol-mediated neuroprotection, we have utilized cultured rat cerebellar neurons. In this system, we previously found that in addition to free radical scavenging, carvedilol may have utility as a low-affinity antagonist of the NMDA* subtype of glutamate receptor channel [8], and as a Na^+ channel blocker to prevent glutamate neurotransmitter release [9].

In the present study, we re-examined the relative potencies of carvedilol and the 3-hydroxylated analogue, SB 211475, as potential neuroprotectants of cultured neurons exposed to three unique systems that elicit cell death. We provide additional new data as well as a statistical re-analysis of previously obtained data. We found that SB 211475 was far more potent as a protective antioxidant, while on the other hand, carvedilol was the more potent neuroprotectant against channel-related neurotoxic events. To determine a biochemical rationale for this interesting dichotomy, we utilized small angle x-ray scattering studies of each compound inserted into both brain membrane lipid and POPC model lipid bilayers. We also determined the relative inhibition of selected DHP calcium channel blockers at neuronal Na^+ channels, showed a correlation between potency and high ClogP values, and determined DHP membrane location by utilizing small angle x-ray scattering studies for comparison with carvedilol and SB 211475. As a result of our studies, we propose that the differential activities of carvedilol and SB 211475 as well as the DHP class of calcium channel blocker may result from the variations in the physical site that each molecule occupies within the plasma membrane bilayer.

MATERIALS AND METHODS

Neuron Culture and Toxicity Assays

Primary cultures of rat cerebellar neurons were prepared from 8-day-old Sprague–Dawley rat pups (Taconic Farms) and used after 8 or 9 days in culture [7–9] by washing and incubating in a buffer composed of (mM): NaCl, 154; KCl, 5.6; $CaCl_2$, 2.3; $MgCl_2$, 1.0; glucose, 5.6; and HEPES, 8.6, adjusted to pH 7.4 with NaOH. For free radical- or glutamate-mediated toxicity, granule cell death is dependent upon the cellular energy state, and occurs in buffer deprived of glucose [10]. For free radical-mediated toxicity, neurons grown in 35-mm dishes were deprived of glucose for 40 min and exposed for 20 min to the hydroxyl radical ($OH^\bullet$) generating system DHF-Fe^{3+}/ADP, with final concentrations of 0.83 mM dihydroxyfumarate, 0.025 mM $FeCl_3$, and 0.25 mM adenosine diphosphate [7]. After challenge, the $OH^\bullet$ generating system was replaced with fresh, glucose-free buffer, and cell death was quantified after 50–60 min by visually counting neurons stained with the vital dye fluorescein diacetate [10]. Results are expressed as percent viability of untreated neurons. To prevent free radical-mediated toxicity, SB 211475 was added to neurons from a concentrated stock in DMSO, 15 min before the oxidative stress. Equivalent amounts of the DMSO vehicle had no protective effect in this system.

To study glutamate-mediated excitotoxicity, cerebellar granule cells were washed in the above glucose-free buffer prior to being exposed to 50 μM glutamate [7, 10]. To prevent glutamate excitotoxicity, SB 211475 was added in increasing concentrations 15 min before the addition of glutamate. Cell death was determined as above after 30 min.

Veratridine is toxic to cultured cells by activating voltage-dependent Na^+ channels and slowing or blocking inactivation. Granule cell death induced by veratridine is not dependent on the cellular energy state, and it occurs in buffer containing glucose [9]. SB 211475 was added in

* *Abbreviations:* DHP, dihydropyridine; IC_{50}, inhibitory concentration giving 50% inhibition; MLV, multilamellar vesicles; NMDA, *N*-methyl-D-aspartate; $^\bullet O_2^-$, superoxide radical; $OH^\bullet$, hydroxyl radical; PC_{50}, protective concentration giving 50% viability; and POPC, palmitoleic phosphatidylcholine.

increasing concentrations to neurons 15 min before the addition of 40 μM veratridine, and cell death was determined as above after 60 min.

[^{3}H]Aspartate Efflux

Veratridine has also been used to induce excitatory amino acid neurotransmitter release in cultured cerebellar granule cells [9], and we tested the ability of SB 211475 to inhibit this evoked release. Neurons in 35-mm dishes were washed in complete buffer as above and incubated in 1 mL of buffer with 1 μCi of D-2,3-[^{3}H]aspartic acid (NET-581, DuPont NEN Research Products) for 15 min at 37°, as previously described [9]. [^{3}H]D-Aspartate is used as a non-metabolizable substrate of the Na^+-dependent, Ca^{2+}-independent glutamate transporter to label cytosolic re-uptake pools [11]. Data were calculated as percent release of total disintegrations per minute loaded, to calculate percent cumulative release after stimulation [9].

Statistical Analysis and Curve-Fitting

SB 211475 data from all neurotoxicity assays and aspartate release experiments were analyzed by non-linear regression analysis and curve-fitting, utilizing GraphPad Prism™, version 2.0 (GraphPad Software). Binding data from the [^{3}H]MK-801 experiments were processed by LIGAND analysis. Previously obtained carvedilol data from Refs. 7–9 were combined with additional carvedilol data from experiments run alongside those of SB 211475 and re-analyzed by GraphPad Prism™. Comparative statistical analyses between SB 211475 and carvedilol PC_{50} and IC_{50} values were performed with unpaired *t*-tests, utilizing the GraphPad Prism™ statistical package. Significance was accepted at $P < 0.05$.

[^{3}H]MK-801 Binding

We measured the ability of SB 211475 to inhibit [^{3}H]MK-801 binding to NMDA receptors in rat cortical membranes. Well-washed membranes from rat brain cortical hemispheres were prepared as described [8, 12]. For binding assays, membranes were suspended in 5 mM Tris with a Polytron to approximately 1.5 mg protein/mL (Bio-Rad protein assay). Displacement binding assays were performed in triplicate at 25° for 60 min in 13 × 100 mm glass tubes in a total volume of 300 μL containing 150 μg of protein, 30 mM $MgCl_2$, 100 μM glycine, 100 μM L-glutamate, and various amounts of SB 211475, with a final concentration of 5 nM [^{3}H]MK-801 to initiate the assay. Membrane-bound radioactivity was separated from free ligand by adding 5 mL of ice-cold assay buffer and filtering through GF/C filters [presoaked in 0.3% (w/v) polyethylenimine], using a Brandel cell harvester and an additional two washes. Liquid scintillation data were analyzed by LIGAND analysis, and the results are expressed as the K_i for SB 211475.

Preparation of Samples for X-Ray Diffraction Studies

POPC and PBPC were purchased from Avanti Polar Lipids. The fatty acid composition of the PBPC lipids included 16:0 (30%), 18:1 (30%), 18:0 (14%), 18:2 (9%), 20:4 (6%), and 22:6 (3%), as determined by GLC analysis. The overall ratio of saturated to unsaturated fatty acids was 0.8:1. Lipids dissolved in chloroform were dried down under a stream of N_2 gas to a thin film in a test tube while vortexing, and residual solvent was removed by vacuum. Buffer (0.5 mM HEPES, 154 mM NaCl, pH 7.3) prepared in the absence or presence of 2% drug (by mass) was added to the lipids while vortexing to yield MLV. Samples for small angle x-ray scattering were prepared by centrifugation of 250 μg of MLV in a Sorvall AH-629 swinging bucket ultracentrifuge rotor (DuPont Corp.) at 35,000 *g* for 90 min at 5° in Lucite sedimentation cells, each containing an aluminum foil substrate. Then samples were placed in brass holders in which the humidity was maintained at 75% with a saturated solution of potassium tartrate.

Small Angle X-Ray Diffraction Data Collection and Analysis

The samples were aligned at near-grazing incidence with respect to the x-ray beam. The radiation source was a collimated, monochromatic x-ray beam (CuKα x-ray, λ = 1.54Å) from a Rigaku RU-200 high brilliance rotating anode x-ray generator (Rigaku U.S.A.). The diffraction data were collected on a one-dimensional position-sensitive electronic detector (Innovative Technologies, Inc.). Data collection and analysis were carried out as previously described [13].

ClogP Determinations

The determination of a ClogP value for a compound allows an estimation of the octanol:water partition coefficient in order to determine the degree of lipophilicity. Therefore, it can determine the extent to which a molecule will intercalate or interact with biologic membranes or model lipid bilayers. We determined ClogP values by using the ClogP Program, version 4.51, distributed by Daylight Chemical Information Systems, Inc. and developed by the Pomona College Medicinal Chemistry Project.

RESULTS

Free Radical Toxicity

Cultured cerebellar granule cell neurons were very sensitive to the toxic action of the free radical generating system, DHF-Fe^{3+}/ADP, which generates superoxide anion ($^{\bullet}O_2^-$) and $OH^{\bullet}$ [14]. SB 211475 was a potent inhibitor with a PC_{50} of 183 nM (Fig. 2). Since we have demonstrated previously that carvedilol can accumulate in neuronal membranes to increase efficacy [7], we grew neurons in the presence of SB 211475 for 4 days, and then tested for free

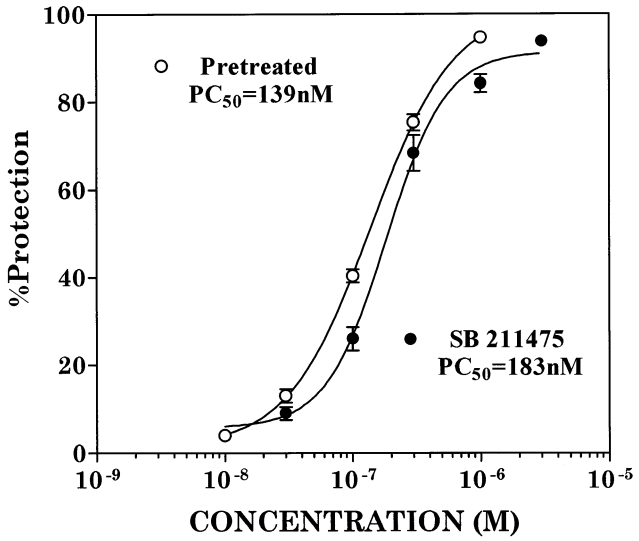

FIG. 2. Protection from oxygen free radical-induced toxicity in cultured rat cerebellar granule cells. Cultured neurons in glucose-free buffer were incubated for 20 min with the $OH^{\bullet}$ generating system, DHF-Fe^{3+}/ADP. SB 211475 was added in increasing concentrations 15 min before the oxidative stress. In the pretreatment model, neurons were also grown in the presence of increasing concentrations of SB 211475 for 4 days prior to the experiment. Cell death was quantitated after 50 min by visually counting neurons stained with fluorescein diacetate. Cell death in buffer control dishes (average of three fields of 100 cells) was < 5% of untreated cells. A PC_{50} of 183 ± 22 nM was determined for SB 211475 (values are the means ± SEM, N = 10). A portion of this total was re-analyzed from ref. 6 (N = 3). Pretreatment for 4 days with SB 211475 lowered the PC_{50} to 139 nM (value is the mean ± 7.8 nM SEM, N = 4), but this difference was not statistically significant.

radical toxicity. As shown in Fig. 2, SB 211475 was slightly more protective with this procedure, yielding a PC_{50} of 139 nM, but this was not a statistically significant difference. In comparison with previous results, SB 211475 was 28-fold more potent than carvedilol against free radical-mediated neurotoxicity (Table 1).

Glutamate-mediated Excitotoxicity

Glutamate is excitotoxic to energy-stressed cerebellar granule cells [10]. SB 211475 protected against glutamate-induced excitotoxicity with a PC_{50} of 7.1 μM (Fig. 3A), which was nearly 6-fold less potent than carvedilol, which showed a PC_{50} of 1.2 μM (Table 1). Since glutamate is excitotoxic to granule cells by interacting at the NMDA receptor, we studied the ability of SB 211474 to inhibit binding of the NMDA receptor ligand, [^{3}H]MK-801, to rat cortical membranes. SB 211475 inhibited [^{3}H]MK-801 binding to rat cortical membranes with a K_i of 110 μM (Fig. 3B), whereas carvedilol competed with a K_i of 29.4 μM (Table 1). Both compounds would be considered low-affinity antagonists; however, they did displace ≥80% of bound ligand. Thus, in both assays that assessed NMDA receptor interaction, SB 211475 was 4- to 6-fold less potent than carvedilol.

Veratridine-mediated Toxicity

Veratridine is toxic to cultured cells by activating voltage-dependent Na^+ channels and slowing or blocking inactivation, causing Na^+ influx and ionic imbalance, resulting in death for cultured cerebellar granule cells within 60 min [9]. SB 211475 concentration-dependently prevented veratridine-mediated neuronal death with a PC_{50} of 920 nM (Fig. 4A) compared with a PC_{50} of 330 nM for carvedilol (Table 1). Veratridine induces excitatory amino acid neurotransmitter release in cultured cerebellar granule cells, and SB 211475 concentration-dependently inhibited the evoked release, with an IC_{50} of 2.6 μM (Fig. 4B). Carvedilol gave an IC_{50} of 1.4 μM in this aspartate release assay (Table 1). Thus, in two different assays to assess inhibition of Na^+ channels, SB 211475 was approximately 2- to 3-fold less potent than carvedilol.

We extended these observations to include the DHP class of voltage-sensitive calcium channel blocker, because these amphipathic molecules are thought to diffuse laterally

TABLE 1. Statistical comparison of the relative potencies of SB 211475 and carvedilol

	Free radical toxicity (PC_{50})	Glutamate toxicity (PC_{50})	[^{3}H]MK-801 binding (K_i)	Veratridine toxicity (PC_{50})	[^{3}H]Aspartate release (IC_{50})
SB 211475	0.183 ± 0.02 μM	7.1 ± 1.6 μM	110 ± 7 μM	0.92 ± 0.14 μM	2.6 ± 0.2 μM
Carvedilol	5.2 ± 0.4 μM*	1.2 ± 0.2 μM†	29.4 ± 2.4 μM‡	0.33 ± 0.02 μM§	1.4 ± 0.18 μM‖
P value	<0.0001	0.0117	<0.0001	0.015	0.006
Response ratio (max/min)	28-fold	5.9-fold	3.7-fold	2.8-fold	1.9-fold

Values are means ± SEM (N = 3–10) and were obtained by non-linear curve fitting, using GraphPad Prism™. Statistical analysis of the data sets were analyzed in GraphPad Prism™ as unpaired *t*-tests.

*Re-analyzed with portions from Ref. 7.

†Re-analyzed from Ref. 7.

‡From Ref. 8.

§Re-analyzed from Ref. 9.

‖Re-analyzed from Ref. 9.

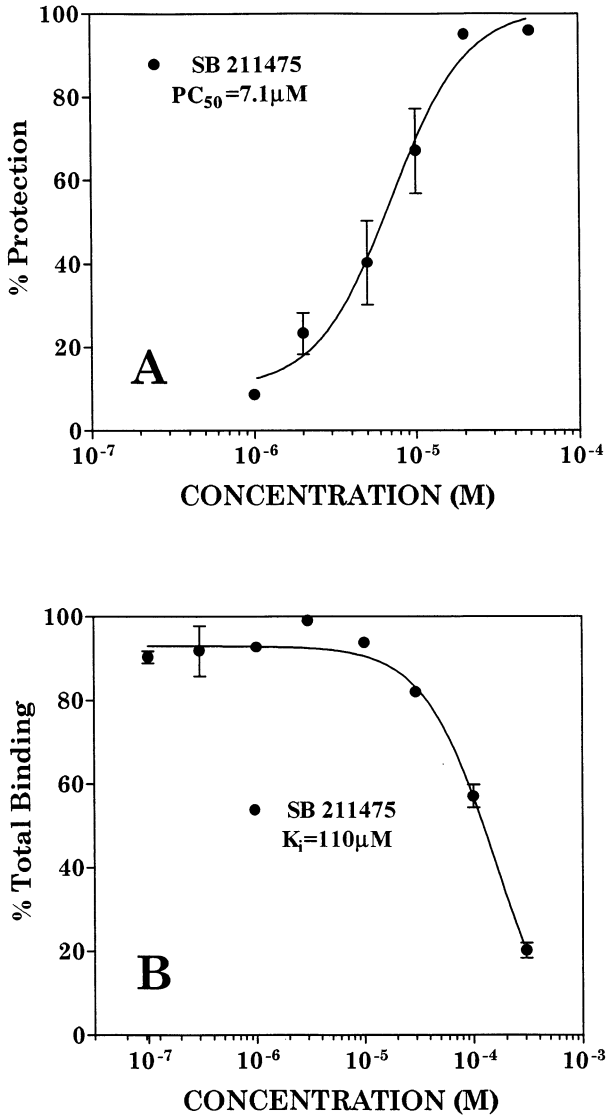

FIG. 3. Comparison of NMDA receptor interaction in cultured rat cerebellar granule cells. (A) SB 211475 was added in increasing concentrations to neurons under energy-stressed conditions, 15 min before the addition of 50 μM glutamate. Cell death was assessed after 30 min by counting neurons stained with the vital dye fluorescein diacetate. Cell death in buffer control dishes (average of three fields of 100 cells) was < 5% of untreated cells. A PC_{50} of 7.1 ± 1.6 μM was determined for SB 211475 (values are means ± SEM, N = 7). (B) [^{3}H]MK-801 displacement studies in rat cortical membranes. Increasing concentrations of SB 211474 were added to membranes before the addition of 5 nM [^{3}H]MK-801. Results are expressed as percent of total binding which averaged 931 ± 101 fmol/mg protein (values are the means ± SEM, N = 3). The average K_i for SB 211474, determined by LIGAND analysis, was 110 ± 6 μM (values are means ± SEM, N = 3).

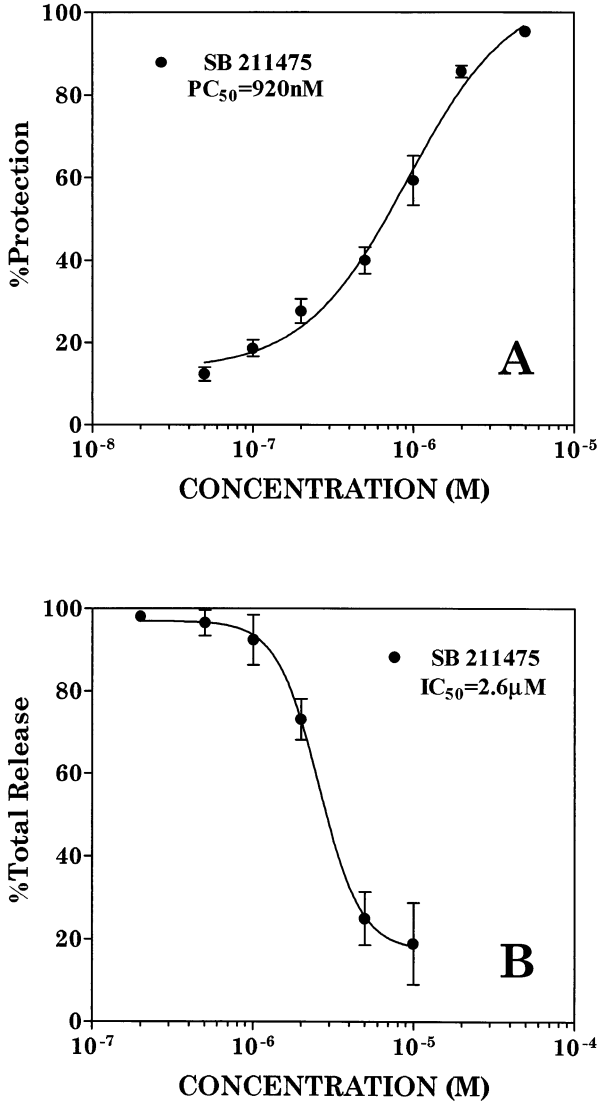

FIG. 4. Comparison of veratridine-mediated actions in cultured rat cerebellar granule cells. (A) SB 211475 was added in increasing concentrations to neurons 15 min before the addition of 40 μM veratridine. Cell death was quantitated after 60 min by visually counting neurons stained with fluorescein diacetate. Cell death in buffer control dishes (average of three fields of 100 cells) was < 5% of untreated cells. A PC_{50} of 920 ± 138 nM was determined for SB 211475 (values are means ± SEM, N = 3). (B) Blockade of veratridine-induced [^{3}H]aspartate release from cultured cerebellar granule cells. The percent release of the total loaded [^{3}H]aspartate (1 μCi) was determined by calculating cumulative release after the addition of veratridine. An IC_{50} of 2.6 ± 0.2 μM was determined for SB 211475 (values are mean ± SEM, N = 6).

within membrane bilayers before binding to the target receptor [15, 16]. We examined four different DHPs in the neuronal aspartate release assay, and the results are presented in Table 2. Flunarizine was found to be the most potent DHP examined, with an IC_{50} of 0.6 μM. We also calculated logP values for these compounds, and it can be seen that flunarizine is also the most lipophilic compound tested, with a ClogP value of 6.424 (Table 2). In comparison, nifedipine showed weak inhibition of aspartate release with an IC_{50} of 84 μM, and was the least lipophilic compound tested, with a ClogP value of 2.353 (Table 2). The other DHPs gave intermediate values that, plotted together, showed a distinct correlation between log IC_{50} and ClogP (r^2 = 0.94).

TABLE 2. Comparison of the relative potencies of selected DHPs

	[^{3}H]Aspartate release (IC_{50})*	ClogP†
Flunarizine	0.6 ± 0.1 μM	6.424
Nicardipine	2.8 ± 0.2 μM	4.221
Isradipine	19 ± 1.1 μM	3.144
Nifedipine	84 ± 7 μM	2.353

*Values are means ± SEM (N = 3) and were obtained by non-linear curve-fitting using GraphPad Prism™.

†Calculated from the ClogP Program, version 4.51, distributed by Daylight Chemical Information Systems, Inc.

Small Angle X-Ray Scattering

We used small angle x-ray scattering to study how the structural properties of model bilayers were altered by the inclusion of either carvedilol or SB 211475. Small angle x-ray scattering data from oriented POPC bilayers prepared in the presence or absence of carvedilol or SB 211475 produced four strong diffraction orders at 20° (Table 3). The unit cell periodicity, or *d*-space (the distance from the center of one membrane to the next, including surface hydration), for the control was 53.7 ± 0.3 Å (Table 3). Following addition of carvedilol or SB 211475 at a 2% (w/w) drug/lipid mass ratio, the *d*-space values were not altered significantly (Table 3). One-dimensional electron density profiles generated from the x-ray diffraction data demonstrated a centrosymmetric membrane bilayer structure (Fig. 5). The two peaks of electron density on either side of the figures correspond to phospholipid headgroups, while the minimum of electron density at the center of the membrane is associated with the terminal methyl groups of the phospholipid hydrocarbon chains from both leaflets of the bilayer. The effects of the drugs on the membrane electron density profiles were determined by subtracting the profiles, and are indicated by shaded areas. Positive differences (> 0 relative electron density) correspond to the equilibrium distribution of the drug molecules within the membrane.

We also examined the electron density profiles generated from x-ray scattering data obtained from brain membrane lipid bilayers, and determined in the presence and absence of carvedilol or SB 211475 (Fig. 6, A and B). As shown, we found very similar distribution profiles between compounds tested in the brain membrane lipids and those obtained with POPC bilayers (Fig. 5, A and B). In both model systems, only carvedilol occupied two distinct locations within the bilayer, one at the hydrocarbon core/glycerol backbone, and one at the hydrophilic surface interface.

For comparison with another class of compounds, we performed small angle x-ray scattering experiments with the DHPs listed in Table 2 to study how their differential Na^+ channel activity might be influenced by their location within brain lipid membranes. As seen in Fig. 7, all DHPs showed electron density profiles that localized them primarily to the glycerol backbone/hydrocarbon interface. The most significant differentiating characteristic among these spectra was that the time-averaged equilibrium location of the most potent molecule, flunarizine, extended to the hydrated surface of the membrane bilayer, seen at ± 22–27 Å (Fig. 7A). A reduction in electron density in this ± 22–27 Å region was clearly seen for nicardipine (Fig. 7B) and was absent for isradipine (Fig. 7C). These spectra demonstrated that those DHPs that were the more mobile or less spatially restricted molecules and had the higher ClogP values were those that were more inhibitory to Na^+ channel activity. On the other hand, the less inhibitory the molecules at Na^+ channels, the less lipophilic they were, with lower ClogP values, and the less the spectra of the compounds showed extension to the hydrated surface of the bilayer.

Interpretation of Electron Density Profiles

The presence of carvedilol produced a broad increase in electron density (± 8–27 Å) from the center of the membrane bilayer, indicating that the time-averaged equilibrium location of carvedilol is within the hydrocarbon core/glycerol backbone and extends to the hydrated surface of the membrane bilayer (Fig. 5A). By contrast, the presence of SB 211475 produced an increase in electron density that was restricted primarily to the hydrocarbon core/glycerol backbone region of the membrane, ± 10–20 Å from the center of the membrane (Fig. 5B). By measuring the distance between the two highest peaks of electron density on either side of the figure, we determined that SB

TABLE 3. Uncorrected normalized intensities for POPC membranes ± carvedilol or SB 211475

Order number	Control for carvedilol	Carvedilol 2% by mass	Control for SB 211475	SB 211475 2% by mass
1	913,000 ± 57,800	927,000 ± 56,000	902,000 ± 60,200	872,000 ± 35,000
2	13,700 ± 921	22,300 ± 1,940	16,000 ± 935	45,200 ± 7,180
3	33,400 ± 2,260	29,700 ± 1,910	35,600 ± 2,780	55,200 ± 3,340
4	39,500 ± 5,120	21,100 ± 3,670	46,000 ± 3,850	27,800 ± 4,350
	d = 53.7 ± 0.3 Å	d = 53.5 ± 0.3 Å	d = 53.9 ± 0.3 Å	d = 53.7 ± 0.3 Å

Small angle x-ray diffraction analysis of oriented POPC membranes resulted in four reproducible diffraction orders at 20°. These data are presented as an average ± SD of three repeated analyses, and were used to generate electron density profiles as shown in Fig. 5. The unit cell periodicity, or *d*-space (the distance from the center of one membrane to the next, including surface hydration), was not altered significantly by the addition of either carvedilol or SB 211475.

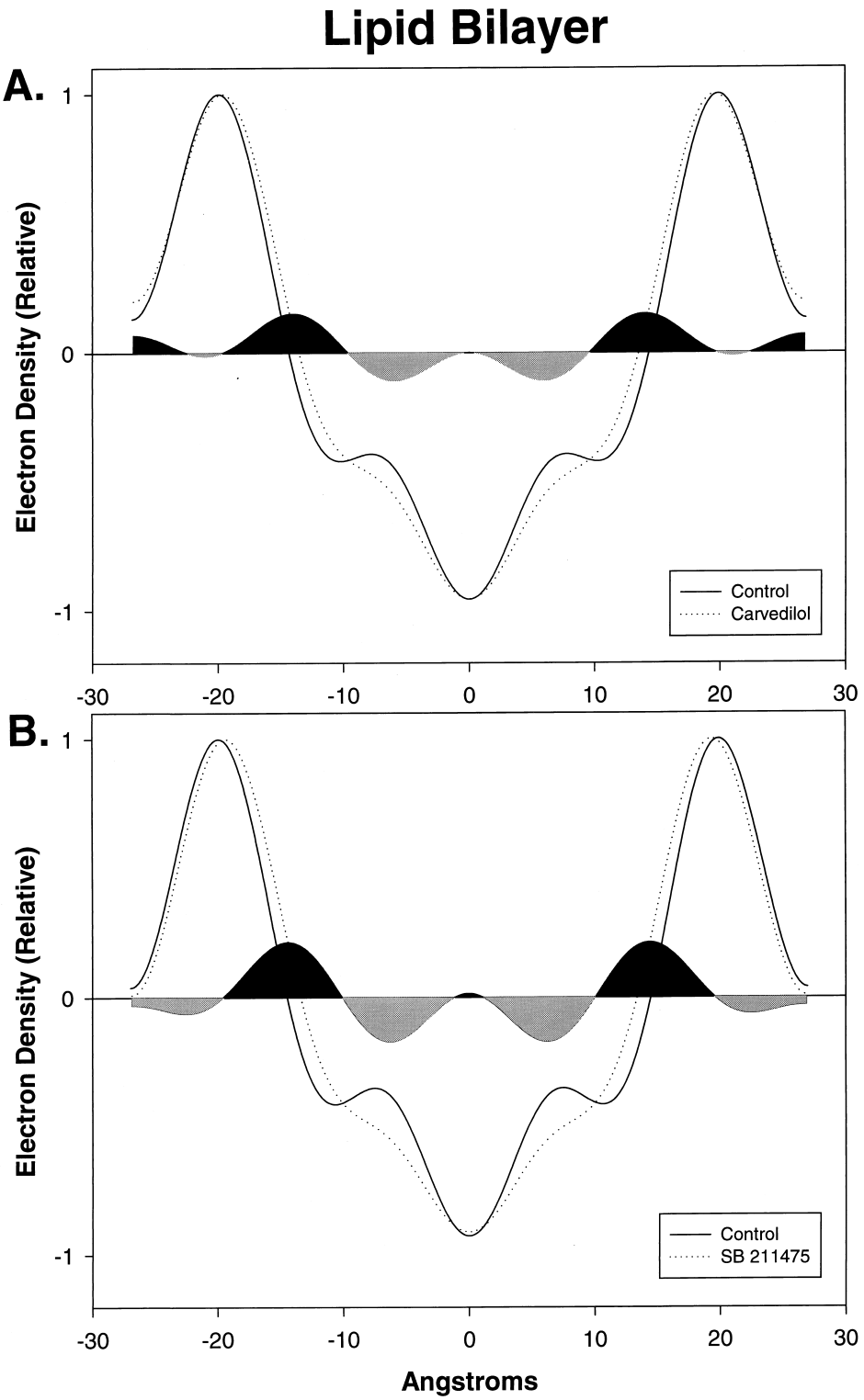

FIG. 5. Lipid bilayer electron density profiles generated from x-ray diffraction analysis. (A) The upper panel shows electron density profiles for POPC oriented membrane multilayers in the absence (solid line) and presence (dashed line) of carvedilol. The effects of carvedilol on the membrane electron density profile were determined by subtracting the profiles, and are indicated by the black shaded areas. The addition of carvedilol produced a broad increase in electron density within the hydrocarbon core/glycerol backbone, and extended to the bilayer surface (positive density). Decreases of electron density (below 0, gray-shaded areas) indicate areas of increased molecular free volume, i.e. increased fluidity. (B) The lower panel shows electron density profiles for POPC oriented membrane multilayers in the absence (solid line) and presence (dashed line) of SB 211475. The addition of SB 211475 produced a broad increase in electron density only within the hydrocarbon core/glycerol backbone, and also reduced the intrabilayer headgroup separation (membrane width) by 2 Å (inward shift at ± 18 Å). This decrease in membrane width was not seen with carvedilol.

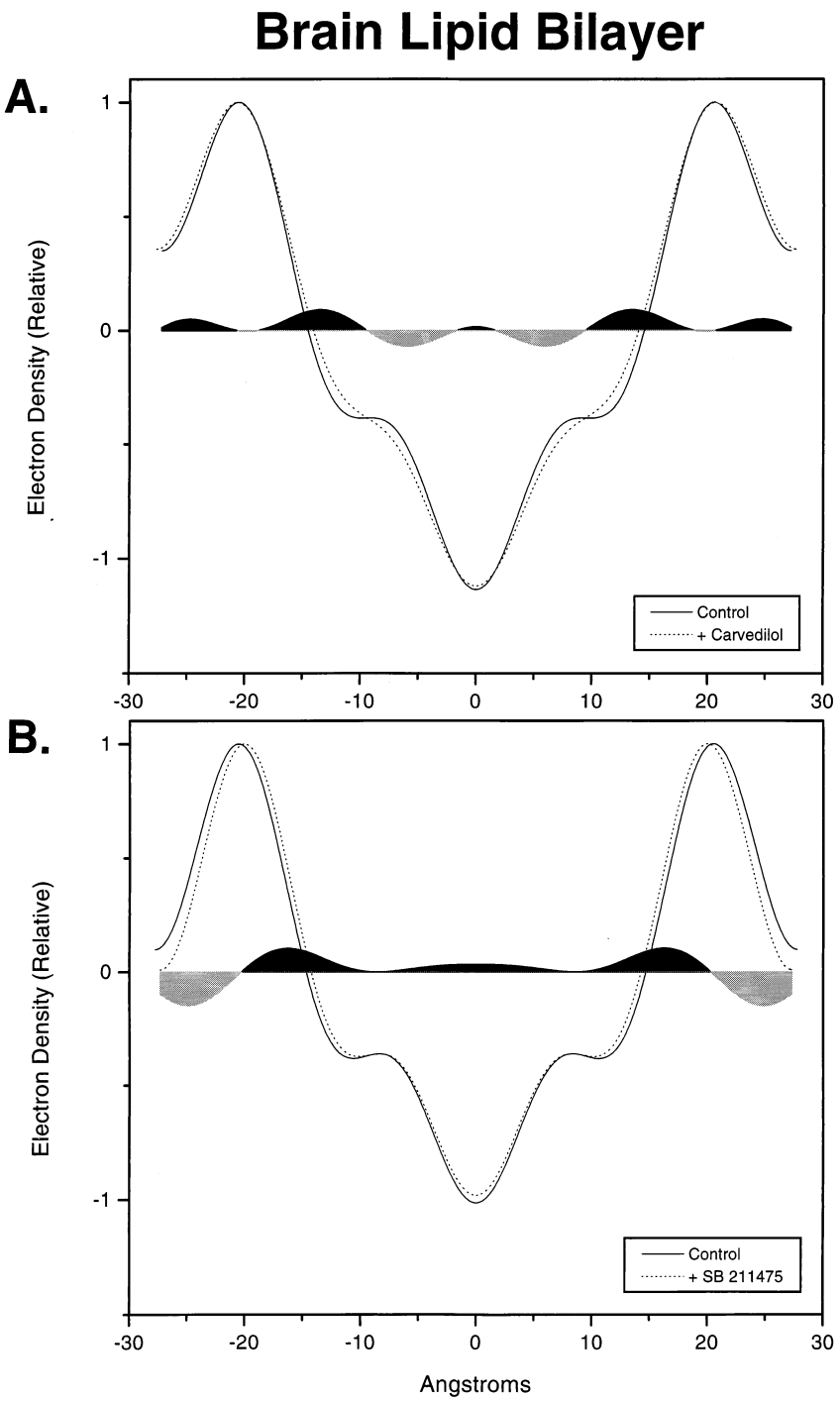

FIG. 6. Brain lipid bilayer electron density profiles generated in the absence and presence of carvedilol or SB 211475. (A) The upper panel shows electron density profiles for brain lipid membrane multilayers in the absence (solid line) and presence (dashed line) of carvedilol. (B) The lower panel shows electron density profiles for brain lipid membrane multilayers in the absence (solid line) and presence (dashed line) of SB 211475. The addition of SB 211475 produced a broad increase in electron density only within the hydrocarbon core/glycerol backbone, and also reduced the intrabilayer headgroup separation (membrane width) by 2 Å (inward shift at ± 20 Å). This decrease in membrane width was not seen with carvedilol.

211475 also reduced the intrabilayer phospholipid headgroup separation by 5% (2 Å), as compared with the control membrane (seen as an inward dotted line shift, Figs. 5B and 6B). This change was not observed with carvedilol or the DHPs (Fig. 7), but this effect of SB 211475 was seen in both POPC and brain lipid model bilayers. This marked reduction in membrane width is consistent with an alteration in the conformation (i.e. *trans-gauche* isomerizations) of the phospholipid acyl chains as a result of the intercalation of SB 211475 into the hydrocarbon core/water interface of the membrane bilayer, a region characterized by high molecular density. Supportive evidence for an interdigitation of SB 211475 among the fatty acyl chains is also seen as a broad, flat, positive electron density at ± 8 Å for SB 211475 in brain lipid bilayers (Fig. 6B), indicative of additional membrane interactions that appear to be unique among the compounds tested. The proposed interaction of SB 211475, showing an alteration in the packing of the acyl chains within a phospholipid monolayer, is presented as a schematic in Fig. 8.

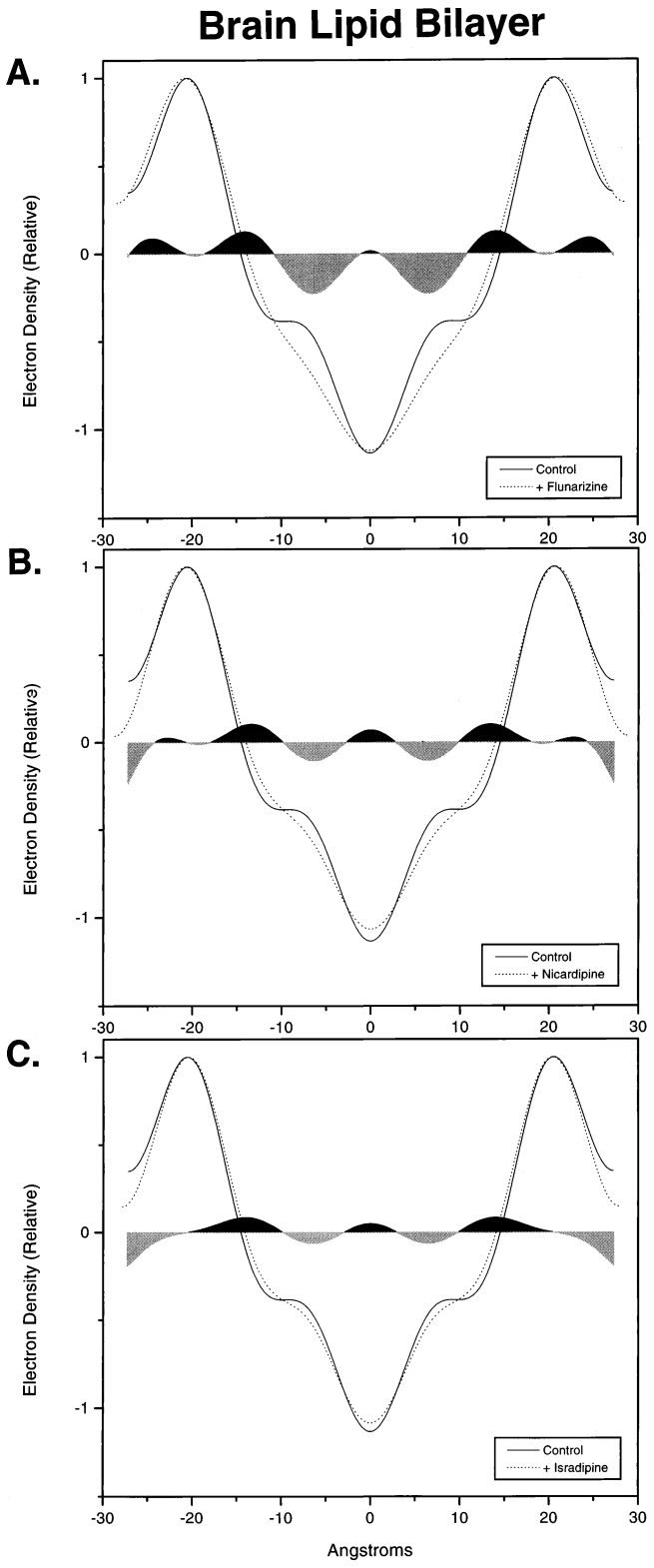

FIG. 7. Brain lipid bilayer electron density profiles generated in the absence and presence of DHPs. The panels show electron density profiles for brain lipid membrane multilayers in the absence (solid line) and presence (dashed line) of selected dihydropyridine calcium channel blockers. The effects of DHPs on the membrane electron density profiles were determined by subtracting the profiles, and are indicated by the black shaded areas. The addition of DHPs produced a broad increase in electron density within the hydrocarbon core/glycerol backbone, but only some compounds showed an extended location to the bilayer surface [seen in (A) for flunarizine at ± 22–27 Å]. Levels of electron density in this region show that flunarizine (A) > nicardipine (B) > isradipine (C), and demonstrate the same order as given by ClogP values (Table 2).

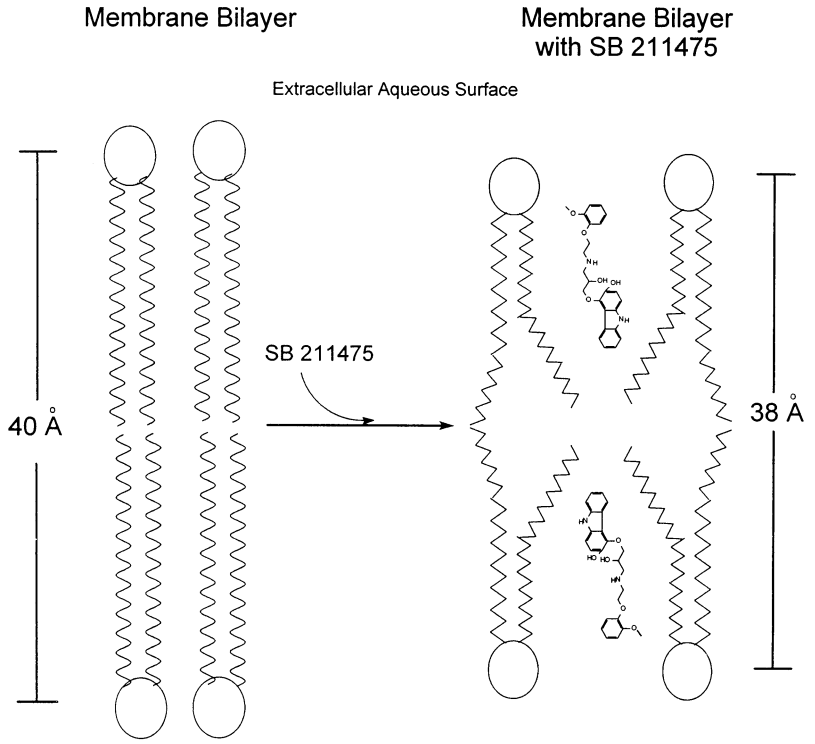

FIG. 8. Molecular model of SB 211475: Effect on membrane structure. As indicated by the x-ray diffraction data, the presence of SB 211475 in the membrane effects a reduction in membrane hydrocarbon core width by 2 Å, most likely by altering the conformation of the phospholipid acyl chains. This effect was not seen with carvedilol.

DISCUSSION

Comparing the three neurotoxicity systems studied here, the greatest difference between the relative potencies of carvedilol and SB 211475 was seen with neuroprotection against oxygen free radical toxicity. This may be a result of molecular positioning of these compounds within the lipid bilayer, or a result of the lower redox potential of SB 211475, which will give it the tendency to donate electrons more readily to "scavenge" the activities of oxygen free radicals [3]. SB 211475 has been shown to be an exceptionally potent antioxidant in a postischemic rat heart model, where its protective action at very low doses was thought to be mediated primarily through a lipid peroxidation chain-breaking mechanism rather than by direct radical scavenging [5]. We have demonstrated in the current study that both compounds insert into model membrane bilayers near the glycerol backbone/hydrocarbon core of the membrane phospholipids. However, whereas the position of carvedilol was less restricted and extended to the hydrated surface of the bilayer, SB 211475 occupied a more limited space at the glycerol backbone/hydrocarbon core, and also decreased the hydrocarbon core width. These studies revealed that SB 211475 may be the superior antioxidant because it likely causes a structural change in its immediate environment to induce a more extensive disordering of phospholipid acyl chains, effectively reducing the rate of free radical chain propagation (Fig. 8).

Previous studies of the effect of lipid physical states on the peroxidation of liposomes demonstrated that lipid peroxidation is promoted in rigid membranes [17] and is diminished in more fluid membranes [18]. Carvedilol has been shown previously to lower the gel to liquid crystalline transition temperature in model liposomal membranes, effectively increasing membrane fluidity [19]. By intercalating into a region of greater molecular density in the membrane bilayer, SB 211475 may promote membrane disorder and fatty acid chain mobility to prevent lipid peroxidation. This contention was further supported by the observed reduction of intrabilayer headgroup separation, which is consistent with a more disordered environment. These findings may be clinically relevant, since SB 211475 is a metabolite of carvedilol in humans (unpublished data).

Carvedilol is a lipophilic compound that is extensively bound to tissues, achieving a high distribution volume of 132 L in humans [20]. It is likely that this protective membrane sequestration results in the biophysical effects shown here, which may augment the pharmacological utilities of this class of compounds. It is known that many lipophilic drugs such as probucol, as well as vitamin E, prevent peroxidative damage to membranes through membrane-active physical effects that supplement chemical activities [21, 22]. Physical effects that supplement chemical activities are particularly evident for DHPs, which modulate Ca^{2+} channels [13, 23]. A membrane pathway for DHPs has been proposed, where receptor binding is preceded by molecular partitioning and lateral diffusion through the lipid bilayer to the target receptor [15, 16]. The concentrations of DHPs achieved in the membrane can be three orders of magnitude greater than in the aqueous environment, and could constitute an augmented receptor affinity characterized by a rapid on-rate and slow off-rate [24].

It is noteworthy that the ClogP values determined for the DHPs used in the present study are correlated with their inhibitory potencies at Na^+ channels. By analogy to these compounds, we calculated the ClogP value to be 3.841 for carvedilol, and 3.033 for SB 211475. These values also correlate with their relative potencies in the aspartate release assay, with an IC_{50} of 1.4 μM for carvedilol and an IC_{50} of 2.6 μM for SB 211475. Therefore, the degree of lipophilicity evidenced by these amphipathic molecules determines, to a certain extent, their relative effectiveness. It is unknown to what extent a "membrane pathway" for carvedilol may figure in its interaction at adrenergic receptors. However, the ligand binding site for the β-adrenergic receptor is within the transmembrane region and is dependent upon critical hydrophobic residues [25]. Furthermore, enhanced adrenergic stimulation has been noted for cholesterol-enriched arteries, by virtue of altering the physical state of vascular smooth muscle membranes by insertion of cholesterol into the lipid bilayer [26].

By analogy to Ca^{2+} channels, both receptor-operated NMDA channels and voltage-sensitive Na^+ channels are use-dependent channels, where opening of the channel is necessary for non-competitive blockade [27]. Carvedilol is likely to be more potent than SB 211475 at channel blockade, as shown in this report, because the entire extent of the receptor channel complex would be more accessible to carvedilol than to SB 211475. We have shown here that carvedilol occupies space at the hydrated surface of the membrane, whereas SB 211475 is more localized to the glycerol backbone/hydrocarbon core. This relationship is also the case for the DHPs studied here; as shown by their electron density profiles, the molecules that were less spatially restricted within the membrane and extended to the hydrophilic interface, and that had the higher ClogP values, were the more potent against Na^+ channel activity.

Veratridine is toxic to cultured cells by acting as a Na^+ channel agonist, causing Na^+ influx and ionic imbalance. Veratridine is a lipophilic molecule, and it mediates neuronal death by Na^+ channel activation at site II, deep within the lipid bilayer [28]. Therefore, the inhibition of veratridine-mediated events by the compounds examined here is likely to be a reflection of their mobility within the hydrocarbon interior, as determined by their lipophilicity (ClogP values). However, the classic Na^+ channel blocker tetrodotoxin is far more potent in this neuronal system, with a PC_{50} of 22 nM and an IC_{50} of 60 nM [29]. Significantly, tetrodotoxin is a site I blocker that interacts at the hydrated outer surface of the plasma membrane channel to interfere directly with channel conductance [28].

Therefore, in addition to its ability to offer protection from myocardial ischemia by virtue of β-blockade, vasodilation, and free radical scavenging, carvedilol and its metabolites may have additional therapeutic value to reduce the risk of cerebral ischemia and stroke. These unique compounds may not only provide protection against stroke by reducing hypertension, the major risk factor, but they may also provide neuroprotection from ischemia-induced excitotoxicity [30]. In addition to acting as a free radical scavenger, sodium channel blocker, and non-competitive antagonist of the NMDA subclass of glutamate receptors, carvedilol and its metabolites may have a membrane-fluidizing effect. As shown here by the x-ray diffraction data, the distinct membrane interaction of these compounds may contribute to our understanding of their neuroprotective mechanisms of action.

References

1. Feuerstein GZ, Hamburger SA, Smith EF III, Bril A and Ruffolo RR Jr, Myocardial protection with carvedilol. *J Cardiovasc Pharmacol* **19:** S138–S141, 1992.
2. Yue T–L, Liu T and Feuerstein G, Carvedilol, a new vasodilator and β-adrenoceptor antagonist, inhibits oxygen-radical-mediated lipid peroxidation in swine ventricular membranes. *Pharmacol Commun* **1:** 27–35, 1992.
3. Yue TL, Cheng HY, Lysko PG, McKenna PJ, Feuerstein R, Gu JL, Lysko KA, Davis LL and Feuerstein G, Carvedilol, a new vasodilator and β-adrenoceptor antagonist, is an antioxidant and free radical scavenger. *J Pharmacol Exp Ther* **263:** 92–98, 1992.
4. Yue T–L, McKenna PJ, Gu J-L, Cheng H–Y, Ruffolo RR Jr and Feuerstein GZ, Carvedilol, a new vasodilating β-adrenoceptor blocker antihypertensive drug, protects endothelial cells from damage initiated by xanthine–xanthine oxidase and neutrophils. *Cardiovasc Res* **28:** 400–406, 1994.
5. Kramer JH and Weglicki WB, A hydroxylated analog of the β-adrenoceptor antagonist, carvedilol, affords exceptional antioxidant protection to postischemic rat hearts. *Free Radic Biol Med* **21:** 813–825, 1996.
6. Yue T–L, McKenna PJ, Lysko PG, Gu J–L, Lysko KA, Ruffolo RR Jr and Feuerstein GZ, SB 211475, a metabolite of carvedilol, a novel antihypertensive agent, is a potent antioxidant. *Eur J Pharmacol* **251:** 237–243, 1994.
7. Lysko PG, Lysko KA, Yue TL, Webb CL, Gu JL and Feuerstein G, Neuroprotective effects of carvedilol, a new antihypertensive agent, in cultured rat cerebellar neurons and in gerbil global brain ischemia. *Stroke* **23:** 1630–1636, 1992.
8. Lysko PG, Lysko KA, Webb CL and Feuerstein G, Neuroprotective effects of carvedilol, a new antihypertensive, at the *N*-methyl-D-aspartate receptor. *Neurosci Lett* **148:** 34–38, 1992.
9. Lysko PG, Webb CL and Feuerstein G, Neuroprotective effects of carvedilol, a new antihypertensive, as a Na^+ channel modulator and glutamate transport inhibitor. *Neurosci Lett* **171:** 77–80, 1994.
10. Lysko PG, Cox JA, Vigano MA and Henneberry RC, Excitatory amino acid neurotoxicity at the *N*-methyl-D-aspartate receptor in cultured neurons: Pharmacological characterization. *Brain Res* **499:** 258–266, 1989.
11. Nichols D and Attwell D, The release and uptake of excitatory amino acids. *Trends Pharmacol Sci* **A Special Report:** 68–74, 1991.
12. Reynolds IJ, Murphy SN and Miller RJ, ^{3}H-Labeled MK-801 binding to the excitatory amino acid receptor complex from rat brain is enhanced by glycine. *Proc Natl Acad Sci USA* **84:** 7744–7748, 1987.
13. Mason RP, Gonye GE, Chester DW and Herbette LG, Partitioning and location of Bay K 8644, 1,4-dihydropyridine calcium channel agonist, in model and biologic membranes. *Biophys J* **55:** 769–778, 1989.
14. Mak IT and Weglicki WB, Protection by β-blocking agents

against free radical-mediated sarcolemmal lipid peroxidation. *Circ Res* **63:** 262–266, 1988.
15. Rhodes DG, Sarmiento JG and Herbette LG, Kinetics of binding of membrane-active drugs to receptor sites. Diffusion-limited rates for a membrane bilayer approach of 1,4-dihydropyridine calcium channel antagonists to their active site. *Mol Pharmacol* **27:** 612–623, 1985.
16. Herbette LG, Vant Erve YM and Rhodes DG, Interaction of 1,4 dihydropyridine calcium channel antagonists with biologic membranes: Lipid bilayer partitioning could occur before drug binding to receptors. *J Mol Cell Cardiol* **21:** 187–201, 1989.
17. McLean LR and Hagaman KA, Effect of lipid physical state on the rate of peroxidation of liposomes. *Free Radic Biol Med* **12:** 113–119, 1992.
18. Mowri H, Nojima S, and Inoue K, Effect of lipid composition of liposomes on their sensitivity to peroxidation. *J Biochem (Tokyo)* **95:** 551–558, 1984.
19. Cheng HY, Randall CS, Holl WW, Constantinides PP, Yue T–L and Feuerstein GZ, Carvedilol-liposome interaction: Evidence for strong association with the hydrophobic region of the lipid bilayers. *Biochim Biophys Acta* **1284:** 20–28, 1996.
20. Neugebauer G, Akpan W, Mollendorf EV, Neubert P and Reiff K, Pharmacokinetics and disposition of carvedilol in humans. *J Cardiovasc Pharmacol* **10:** S85–S88, 1987.
21. McLean LR, Thomas CE, Weintraub B and Hagaman KA, Modulation of the physical state of cellular cholesteryl esters by 4,4′-(isopropylidenedithio)bis(2,6-di-*t*-butylphenol) (Probucol). *J Biol Chem* **267:** 12291–12298, 1992.
22. Lucy JA, Functional and structural aspects of biologic membranes. A suggested role for vitamin E in the control of membrane permeability and stability. *Ann NY Acad Sci* **203:** 4–11, 1972.
23. Mason RP, Differential effect of cholesterol on membrane interaction of charged versus uncharged 1,4-dihydropyridine calcium channel antagonists: A biophysical analysis. *Cardiovasc Drugs Ther* **9:** 45–54, 1995.
24. Mason RP, Rhodes DG and Herbette LG, Reevaluating equilibrium and kinetic binding parameters for lipophilic drugs based on a structural model for drug interaction with biologic membranes. *J Med Chem* **34:** 869–877, 1991.
25. Strader CD, Sigal IS, Register RB, Candelore MR, Rands E and Dixon RAF, Identification of residues required for ligand binding to the β-adrenergic receptor. *Proc Natl Acad Sci USA* **84:** 4384–4388, 1987.
26. Broderick R, Bialecki R and Tulenko TN, Cholesterol-induced changes in rabbit arterial smooth muscle sensitivity to adrenergic stimulation. *Am J Physiol* **257:** H170–H178, 1989.
27. Rogawski MA, Therapeutic potential of excitatory amino acid antagonists: channel blockers and 2,3-benzodiazepines. *Trends Pharmacol Sci* **14:** 325–331, 1993.
28. Catterall WA, Cellular and molecular biology of voltage-gated sodium channels. *Physiol Rev* **72:** S15–S48, 1992.
29. Lysko PG, Webb CL, Yue T–L, Gu J–L and Feuerstein G, Neuroprotective effects of tetrodotoxin as a Na^+ channel modulator and glutamate release inhibitor in cultured rat cerebellar neurons and in gerbil global brain ischemia. *Stroke* **25:** 2476–2482, 1994.
30. Lysko PG, Feuerstein GZ and Ruffolo RR Jr, Carvedilol—a novel multiple action anti-hypertensive drug. *Pharm News* **2:** 12–16, 1995.